Immunobiology 224 (2019) 355–361

Contents lists available at ScienceDirect

Immunobiology

journal homepage: www.elsevier.com/locate/imbio

Depletion of tumor-associated macrophages enhances the anti-tumor effect of docetaxel in a murine epithelial ovarian cancer

Xiaofen Lu, Tengteng Meng*

Department of Obstetrics and Gynecology, Liaocheng People's Hospital, No. 67, Dongchang West Road, Liaocheng, 252000, Shandong, China

ARTICLE INFO

Keywords:
Tumor-associated macrophages
Docetaxel
Ovarian cancer
Depletion
BLZ945

ABSTRACT

Docetaxel (DTXL), a new member of the taxoid family, has been used for cancer treatment. However, increasing cases of DTXL resistance have been reported. Tumor-associated macrophages (TAMs) have been implicated in tumor invasion and chemo-resistance. Eliminating TAMs by inhibiting colony stimulating factor-1 receptor (CSF-1R) has emerged as a promising strategy for cancer treatment. BLZ945 is a CSF-1R inhibitor and has anti-tumor function. In present study, anti-tumor effects of combination treatment of BLZ945 and DTXL were investigated. We established a mouse ovarian cancer model and investigated the effect of BLZ945, DTXL single treatment or combination treatment on TAMs infiltration, tumor growth, $CD8^+$ T cell infiltration and cancer metastasis. DTXL treatment increased the infiltration while BLZ945 induced cell apoptosis in macrophages. DTXL/BLZ945 combination treatment significantly inhibited tumor growth, reduced the abundance of TAMs, increased $CD8^+$ T cell infiltration and prevented lung metastasis. Depletion of Tumor-Associated Macrophages (TAMs) by BLZ945 enhanced the anti-tumor effect of DTXL in a murine epithelial ovarian cancer.

1. Introduction

Ovarian cancer (OC) is one of the most lethal gynecologic cancer and is the fifth leading cause of cancer death in women (Al-Wahab et al., 2014). In China, OC is the tenth most common cancer in women (Reid et al., 2017). The epithelial ovarian cancer (EOC) accounts for over 95% of the ovarian malignancies and becomes a serious threat to women's lives (Guppy et al., 2005). Treatment of EOC is based on the combination of surgery and chemotherapy. Standard treatment for advanced ovarian cancer in the past three decades includes surgical tumor debulking and following platinum-based chemotherapy (Kim et al., 2012). Surgery is considered the mainstay of treatment for ovarian cancer to reduce the tumor burden to no visible disease and therapeutic strategies include intravenous and IP chemotherapy. Docetaxel (DTXL) belongs to the taxoid family which has shown significant activity in a variety of cancers including breast, lung, ovarian, head and neck, and gastric cancers. DTXL has demonstrated potent both in vitro and in vivo cytotoxic activity against a range of tumor types, particularly ovarian cancer. DTXL functions as a spindle poison which promotes microtubulin assembly and stabilizes the polymer, leading to the inhibition of microtubule dynamics and cell cycle arrest (Katsumata, 2003).

Tumor-associated macrophages (TAMs) are a set of macrophages present in high numbers in the microenvironment of solid tumors, which are heavily involved in cancer-related inflammation. Most evidence has suggested that TAMs have a tumor-promoting phenotype and drive pathological phenomena including tumor cell proliferation, tumor angiogenesis, invasion and metastasis, immunosuppression, and drug resistance (Qian and Pollard, 2010; Mantovani et al., 2017).Therefore, eliminating TAMs has emerged as a hopeful strategy for cancer treatment (Tang et al., 2013; Sica et al., 2006). Recently, selective depletion of TAMs by inhibiting colony stimulating factor-1 (CSF1)/CSF1 receptor (CSF1R) signaling pathway has been reported to improve the efficacy of chemotherapy in mammary tumors (Mitchem et al., 2013). BLZ945 is a CSF-1R inhibitor which has been shown to target TAMs and regress established glioma (Pyonteck et al., 2013). However, the role of BLZ945 in ovarian cancer remains unknown.

In current study, we investigated the effect of TAMs depletion by BLZ945 and the following effect on TAMs and anti-tumor activity of DTXL using a mouse ovarian model.

2. Materials and methods

2.1. Cell culture

ID8 mouse ovarian surface epithelial cells were purchased from

* Corresponding author.
E-mail address: mengtengteng2019@126.com (T. Meng).

https://doi.org/10.1016/j.imbio.2019.03.002
Received 23 February 2019; Received in revised form 13 March 2019; Accepted 18 March 2019
Available online 22 March 2019

Millipore (Shanghai, China) and maintained in DMEM supplemented with 10% heat inactivated fetal bovine serum (FBS), 100 U/ml penicillin, 100 μg/ml streptomycin, 5 μg/ml insulin, 5 μg/ml transferrin, and 5 ng/ml sodium selenite (Roche, Indianapolis, IN, USA) in a 5% CO_2 atmosphere at 37 °C. Bone marrow-derived macrophages (BMDMs) were generated as described previously (Wolf et al., 2011). Briefly, bone marrow cells from femurs and tibias were cultured for 6–7 days in complete RPMI 1640 (10% FBS, 100 U/ml penicillin, 100 mg/ml streptomycin, 2 mM L-glutamine) containing M-CSF (10 ng/ml) in Petri dishes before transfer to tissue culture plates for further analysis. In some experiments, BMDMs were treated with 0.05, 0.25 or 0.5 μM BLZ945 (Cayman Chemical, Ann Arbor, MI, USA) for 24 h. In some experiments, ID8 cells were co-cultured with BMDMs for 24 h. Then cells were treated with 2 μg/mL DTXL or 0.5 μM BLZ945, or combination for 48 h.

2.2. Mice tumors

5×10^6 ID8 mouse ovarian cancer cells in 200 μl phosphate buffer saline (PBS) were injected into 6–8 weeks old female C57BL/6 mice subcutaneously. When the tumor volumes reach about 100 mm^3, the tumor-bearing mice were administrated with 2.5 mg/kg DTXL or PBS (control) every 3 days intravenously. Two days post the 3rd administration, mice were sacrificed and tumor tissues were harvested for analysis. In some experiments, the tumor bearing mice were divided into 4 groups with 8 mice per group: Group1: Control group mice were injected with PBS. Group 2: mice were injected 0.5 mg/kg DTXL intravenously. Group 3: mice were injected with 20 mg/kg BLZ945, Group 4: mice were injected with DTXL and BLZ945. The treatments were administrated every 3 days for total 5 times. The tumor volume and weight were monitored. Animal study was approved by the Ethical Committee of Liaocheng People's Hospital.

2.3. MTT assay

Cell viability was detected using Cell Proliferation Kit I (MTT) (Sigma, St Louis, MO, USA). Briefly, 5000 ID8 cells and BMDMs mixture (with ratio of 5:1) were seeded in each well of 96-well plate and cultured for 24 h. Next day the cells were treated with 2 μg/mL DTXL or 0.5 μM BLZ945, or combination for 48 h. Then cells were incubated with 10 μL MTT labeling reagent and incubated at 37 °C for 4 h. Then 100 μL solubilization solution was added and cells were incubated for overnight. Next day the optical density of each well was read at 570 nm using a microplate reader.

2.4. Flow cytometry

Tumor tissues were harvested and digested with 1 mg/mL collagenase IV to prepare the single-cell suspension. For surface staining, cells were incubated with anti-Fc receptor antibody (clone 2.4G2) (Biolegend, San Diego, CA, USA) and stained with antibodies in staining buffer (PBS containing 2% FBS) on ice for 30 min. The antibodies used in present study were: APC anti-mouse F4/80 Antibody (Biolegend), PerCP/Cyanine5.5 anti-mouse Ly-6 G/Ly-6C (Gr-1) Antibody (Biolegend), FITC anti-mouse CD45 Antibody (Biolegend), FITC anti-mouse CD8a Antibody (Biolegend), Brilliant Violet 421™ anti-mouse CD4 Antibody (Biolegend). The samples were analyzed using a BD LSR Fortessa X-20 cytometer and analyzed with FlowJo software.

2.5. Apoptosis assay

BMDMs were seeded in 6 well plate and treated with 0.05, 0.25 and 0.5 μM BLZ945 for 48 h. Then cells were harvested and stained with fluorescein isothiocyanate (FITC)-conjugated annexin V and propidium iodide (PI) by using the annexin-V-FITC staining kit (ThermoFisher, Waltham, MA, USA). After staining, cells were analyzed in FACSCalibur flow cytometer by using CellQuest 3.0.1 software (BD Biosciences, Franklin Lakes, NJ, USA). Percentages of cells undergoing apoptosis were determined by dual-color analysis using FlowJo.

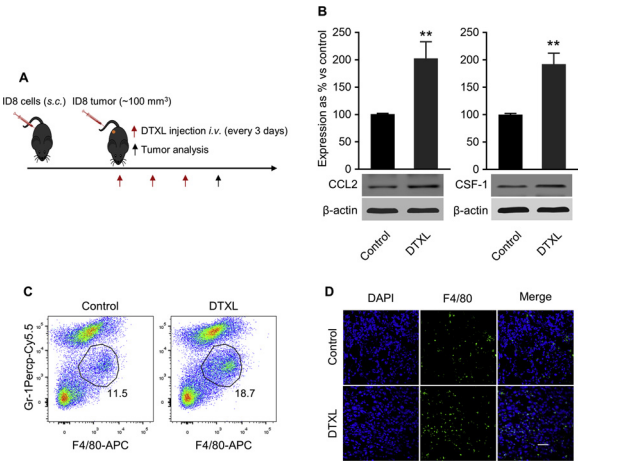

Fig. 1. DTXL treatment increased the infiltration of TAMs in a murine epithelial ovarian ID8 tumor model. (A) Murine epithelial ovarian ID8 tumor models were established by injecting ID8 cells subcutaneously, and tumor-bearing mice were treated with PBS solution or DTXL (2.5 mg/kg) every three days intravenously when the tumor volumes reach about 100 mm3. Two days post third injection, the expression of certain chemokines and abundance of TAMs in tumor tissues were detected. (B) The expression of CCL2 and CSF-1 in tumor tissues after DTXL treatment were examined by Western blotting. β-actin was used as the loading control. **$p < 0.005$. The abundance of TAMs in DTXL-treated mice were detected by flow cytometry (C) and laser scanning confocal microscopy (D). Nuclei were stained by DAPI (blue) and macrophages were stained with anti-F4/80 antibody labeled with FITC (green). Scale bar, 20 μm (For interpretation of the references to colour in this figure legend, the reader is referred to the web version of this article).

2.6. Western blot

Total proteins from tumor tissue were extracted using T-PER™ Tissue Protein Extraction Reagent M-PER® (ThermoFisher). Total proteins from BMDM were extracted using Mammalian Protein Extraction Reagent (ThermoFisher). Protein concentration was measured using Pierce™ BCA Protein Assay Kit (ThermoFisher). Total 25 μg proteins were loaded onto sodium dodecyl sulfate polyacrylamide gel electrophoresis gel and then transferred to polyvinylidene difluoride membrane. The membrane was blocked at room temperature for 1 h by 5% non-fat milk and then incubated with primary antibodies overnight. Next day, membranes were washed with tris-buffered saline buffer containing 0.1% Tween20 for 3 times and then incubated with corresponding horseradish peroxidase-conjugated secondary antibodies for 1 h at room temperature. Primary antibodies used in present study were: anti-CCL2 (Abcam, Cambridge, MA, USA), anti-CSF-1 (Sigma), anti-β actin (Sigma), anti-Phospho-CSF1R (ThermoFisher), anti-VEFG (Santa Cruz, Dallas, TX, USA), anti-MMP9 (Santa Cruz). Clarity™ Western ECL Blotting Substrates (Bio-Rad, Hercules, CA, USA) was used to detect the immunoreactive proteins. The density was quantitated using GS-900™ Calibrated Densitometer (Bio-Rad) and analyzed by using Image Lab (Bio-Rad).

2.7. qRT-PCR

The total RNA from tumor tissue was isolated using an RNeasy Mini kit (Qiagen, Germantown, MD, USA) following the manufacturer's instructions. Reverse transcription was performed using SuperScript® III First-Strand Synthesis System (ThermoFisher). Real time quantitative PCR reactions were set up in triplicate using SYBR® Green Master Mix (Bio-Rad) and run on a QuantStudio 3 Real-Time PCR System

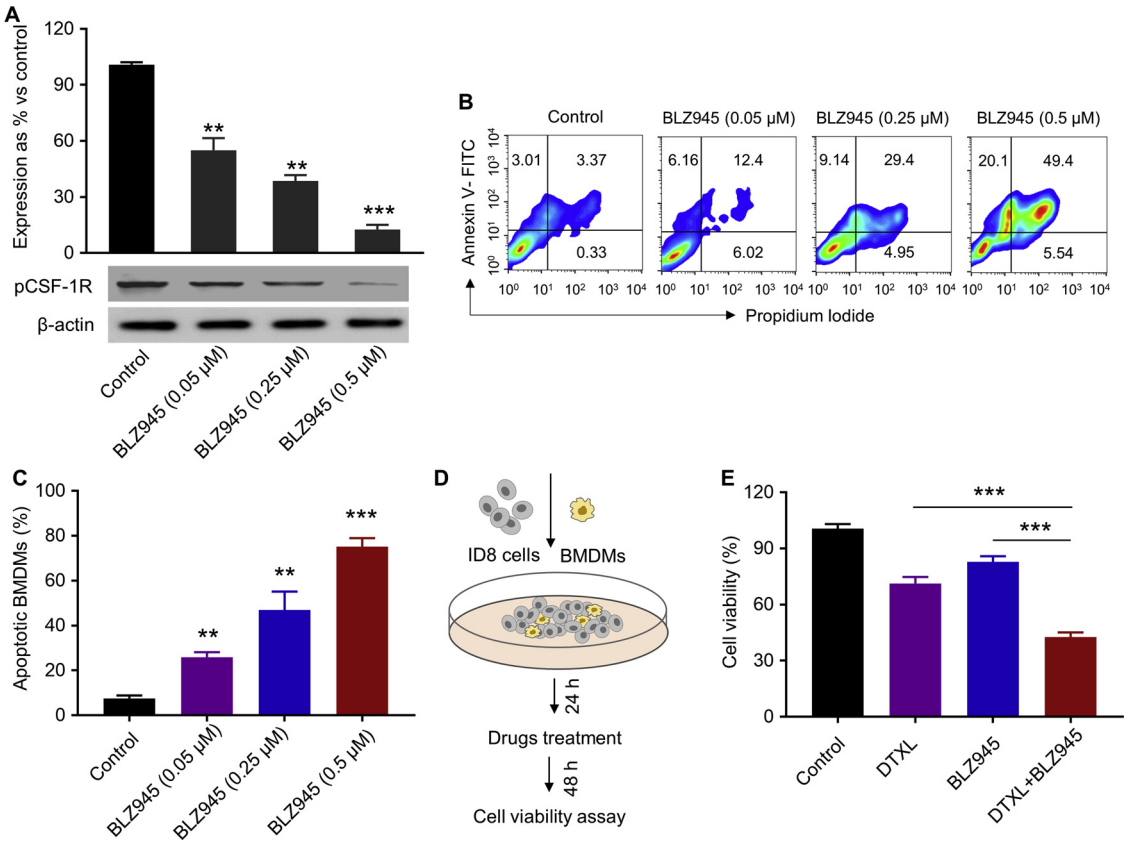

Fig. 2. In vitro therapeutic efficacy of DTXL and BLZ-945. (A) pCSF-1R expression in BMDMs following incubation with different concentrations of BLZ945 for 24 h. BLZ945 was a specific inhibitor of CSF-1R, and CSF-1/CSF-1R pathway plays an essential in the survival of macrophages. Three concentrations of BLZ945 (0.5, 0.25 and 0.5 μM) were set. β-actin was used as the loading control. (B) Apoptosis of BMDMs after treated with different concentrations of BLZ945 for 48 h. Apoptotic BMDMs were detected by double staining with Annexin-V and propidium iodide (PI), and measured by flow cytometry. (C) Bar graph shows the percentage of apoptotic BMDMs after treatment. (D) Scheme of co-culture assay of ID8 cells and BMDMs, co-cultured cells were treated DTXL, BLZ945 or two drugs. (E) Cell viability of co-cultured cells after treated with different drugs were examined by MTT assay. The concentrations of DTXL and BLZ945 were 2 μg/mL and 0.5 μM, respectively. Cell viability was normalized to that of PBS-treated cells which served as the indicator of 100% cell viability. Data represent means ± SD. $^{**}p < 0.005$, $^{***}p < 0.001$.

(ThermoFisher). The following primers were used in the current study: *Arg1* Forward: 5′-GGAATCTGCA TGGGCAACCTGTGT-3′, Reverse: 5′-AGGGTCTACGTCTCGCAAGCCA-3′. *Mrc1* Forward: 5′-GCAAATGGA GCCGTCTGTGC-3′, Reverse: 5′-CTCGTGGATCTCCGTGAC AC-3′. IL-10 Forward: 5′-GCTATGCTGCCTGCTCTTACT-3′, Reverse: 5′-CCTGCTGAT CCTCATGCCA-3′. VEGF Forward: 5′-GTACCTCCACCATGCCAAGT-3′, Reverse: 5′-TCACATCTGCAAGTACGTTCG-3′. MMP9 Forward: 5′-ACG ACATAGACGGCATCCAG TATC-3′, Reverse: 5′-AGGTATA GTGGGACA CATAGTGGG-3′. *GAPDH* Forward: 5′- ACTTTGGCATTGTGGAAGG -3′, Reverse: 5′- ACACATTG GGGGTAGGAACA -3′.

2.8. Hematoxylin and eosin (H&E) staining

The histopathological analysis was performed by using H&E staining. Briefly, after being fixed in 10% formalin, the tumor tissues or lungs were dehydrated and then embedded in paraffin. Then, the paraffin embedded sample was sliced to 5 μm sections, and tissue sections were stained with H&E.

2.9. Immunohistochemistry (IHC) staining

IHC was performed on 5 μm thick formalin-fixed, paraffin-embedded tissue sections mounted on glass slides. After deparaffinization and Ag retrieval treatments, slices were incubated with primary antibodies and detected by streptavidin-peroxidase method or immunofluorescence method. FITC-Anti-F4/80 antibody was purchased from Biolegned and anti-CD8 antibody was purchased from Abcam.

2.10. Statistical analysis

Data were presented as the mean ± SD. One- or two-way ANOVA analysis, followed by a Tukey's post hoc test was used to analyze the data. When $p < 0.05$, the Statistical difference was considered as significant.

3. Results

3.1. DTXL treatment increased the infiltration of TAMs in a murine epithelial ovarian ID8 tumor model

First, we established the murine ovarian tumor model by injecting ID8 cells. Once the tumor reached about 100 mm^3, DTXL was administrated for 3 times (Fig. 1A). CSF-1 and CC chemokine ligand 2 (CCL2) were tumors secrete signaling molecules and attracted monocytes and tissue-resident macrophages, and convert these cells to the cancer-supporting TAM phenotype (Guo et al., 2013). As macrophage infiltration in cancer correlates with high expression of the CCL2 and CSF-1 (Richardsen et al., 2015; Bonapace et al., 2014), we monitored the protein levels of CCL2 and CSF-1 in tumor tissues from DTXL treated or control tumor mice. As shown in Fig. 1B, the levels of both CCL2 and CSF-1 in tumor tissue from DTXL-treated mice were significantly higher than that from PBS-treated control mice, suggesting possible

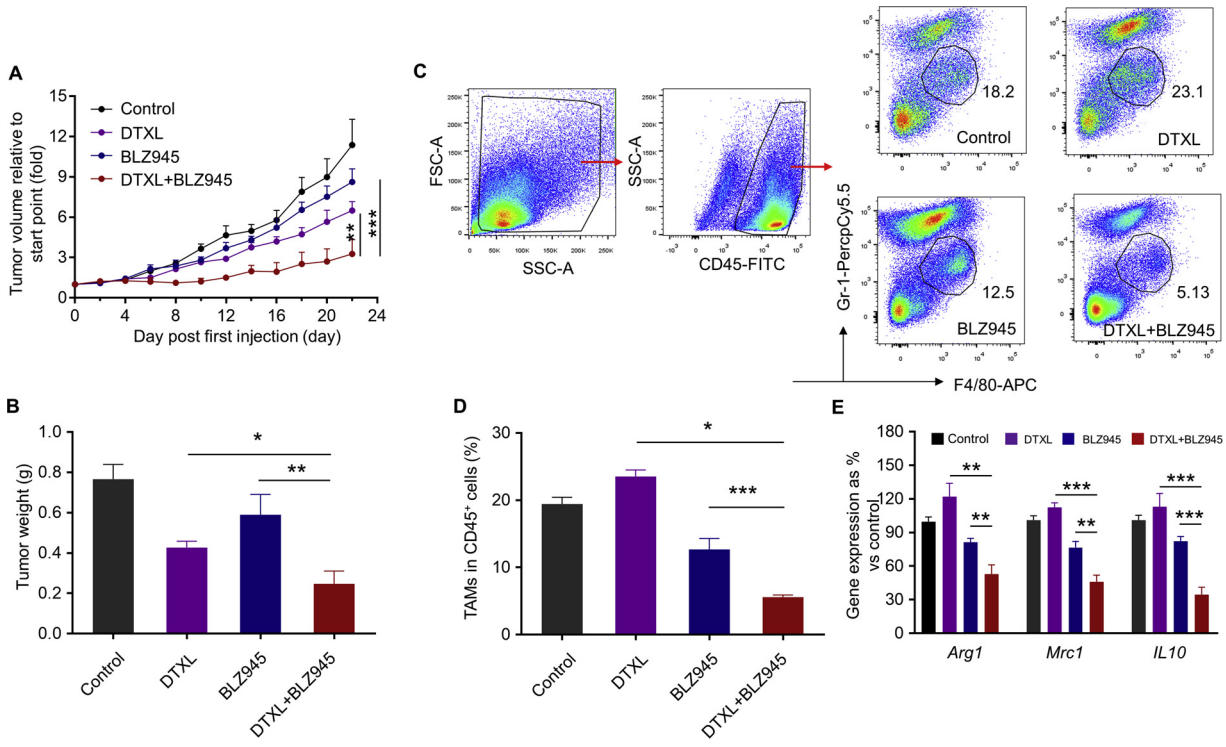

Fig. 3. Combination therapy significantly inhibits tumor growth and reduces the abundance of TAMs in murine ID8 ovarian cancer. (A) Inhibition of tumor growth by various therapeutics in ID8 tumor-bearing C57BL/6 mice (n = 8). The injection dose of DTXL (intravenously, i.v.) and BLZ945 (intraperitoneally, i.p.) were 2.5 mg/kg and 20 mg/kg, respectively. DTXL + BLZ945 versus DTXL, **p < 0.005; DTXL + BLZ945 versus BLZ945, ***p < 0.001. (B) Weight of ID8 xenograft tumors at the final point of treatment. Data are shown as means ± SD (n = 8). *p < 0.05, **p < 0.005. (C) The ratio of Gr-1-F4/80+ TAMs in tumor-infiltrating immune cells at the end of treatment analyzed by flow cytometry. Cells were gated from CD45+ immune cells. (D) Bar graph shows the percentage of TAMs in tumor-infiltrating immune cells. Data are shown as means ± SD (n = 8). *p < 0.05, ***p < 0.001. (E) Expression of mannose receptor-1 (Mrc1), arginase-1 (Arg1) and interleukin 10 (IL10) in tumor tissues after treated with DTXL, BLZ945 or combinations. Data are shown as means ± SD (n = 8). **p < 0.005, ***p < 0.001.

macrophage infiltration in tumor tissue in DTXL-treated tumor mice. We continued to compare the abundance of TAMs in tumor tissues between control and DTXL-treated tumor mice. Based on previous reports, the TAMs were $CD45^+F4/80^+Gr\text{-}1^-$ (DeNardo et al., 2009, 2011. Therefore, we stained the tumor tissue cells with anti-CD45, F4/80 and Gr-1 antibodies. After gating the CD45 positive cells, we compared the abundance of $F4/80^+Gr\text{-}1^-$ cells. As shown in Fig. 1C, the percentage of $F4/80^+Gr\text{-}1^-$ cells in tumor tissue from DTXL-treated tumor mice were higher than that from control tumor mice, indicating increased infiltration of TAMs in DTXL-treated tumor mice. Similarly, we also detected more F4/80 positive cells by immunofluorescence/immunohistochemistry staining in tumor tissues from DTXL-treated tumor mice (Fig. 1D). Taken together, our data indicated that DTXL treatment increased TAMs infiltration in ovarian tumor mice.

3.2. DTXL and BLZ945 efficiently inhibited cell proliferation in vitro

Depletion of TAMs has been shown to enhance anti-tumor immunity (Shen et al., 2014; Dammeijer et al., 2017). BLZ-945 is a CSF-1R inhibitor which selectively binds to CSF1R expressed on TAMs and inhibits proliferation of TAMs (Pyonteck et al., 2013). Therefore, we evaluated the inhibitory efficiency of BLZ945 together with DTXL. First we treated BMDMs with different concentration of BLZ945 and monitored the level of phosphorylated CSF-1R, which was the common marker of CSF1/CSF-1R signaling pathway activation (Stanley and Chitu, 2014). As shown in Fig. 2A, BLZ945 treatment significantly decreased the level of pCSF-1R and the highest concentration 0.5 μM of BLZ945 gave the best inhibitory effect. This data indicated that BLZ-945 inhibited CSF-1R signaling pathway in a dose-dependent manner. Consequently, BLZ-945 treatment increased numbers of Annexin V and PI positive cells in BMDMs (Fig. 2B), indicating BLZ-945 promoted apoptosis in BMDMs (Fig. 2C). Finally, we established the co-cultured the ID8 cells with BMDMs and then treated the cell culture with DTXL, BLZ945 or DTXL/BLZ-945 combination (Fig. 2D) and monitored the cell viability. As shown in Fig. 2E, single treatment of DTXL or BLZ945 decreased the cell viability. Interestingly, DTXL/BLZ945 combination treatment resulted in significantly decreased cell viability when compared to single treatment. Therefore, our data demonstrated that DTXL/BLZ-945 treatment efficiently inhibited cell proliferation *in vitro*.

3.3. DTXL and BLZ945 combination therapy significantly inhibits tumor growth and reduces the abundance of TAMs

We continued to evaluate the effects of DTXL and BLZ945 combination treatment *in vivo*. Tumor bearing mice were injected with 2.5 mg/kg DTXL intravenously or 20 mg/kg BLZ-945 or combination and the tumor volume and weight were measured after treatment. As shown in Fig. 3A, single treatment of DTXL or BLZ945 decreased the tumor volume while the combination treatment displayed a significantly better inhibitory effect on tumor volume when compared to DTXL or BLZ945 single treatment. Similarly, DTXL and BLZ945 combination treatment resulted in significantly decreased tumor weight when compared to single treatment (Fig. 3B). We monitored the TAMs infiltrations in the tumor bearing mice after different treatments (Fig. 3C). We detected increased $CD45^+F4/80^+Gr\text{-}1^-$ cells in DTXL-treated mice, indicating DTXL enhanced TAMs infiltration. The BLZ945 treatment decreased the cell ratio of $CD45^+F4/80^+Gr\text{-}1^-$, indicating BLZ945 reduced TAMs abundance. Interestingly, there was significantly decreased ratio of $CD45^+F4/80^+Gr\text{-}1^-$ in DTXL/BLZ945 combination-treated mice (Fig. 3D), when compared to single-treated mice, indicating DTXL/BLZ945 treatment significantly reduced the TAMs abundance in tumor bearing mice. Correspondingly, DTXL/BLZ945

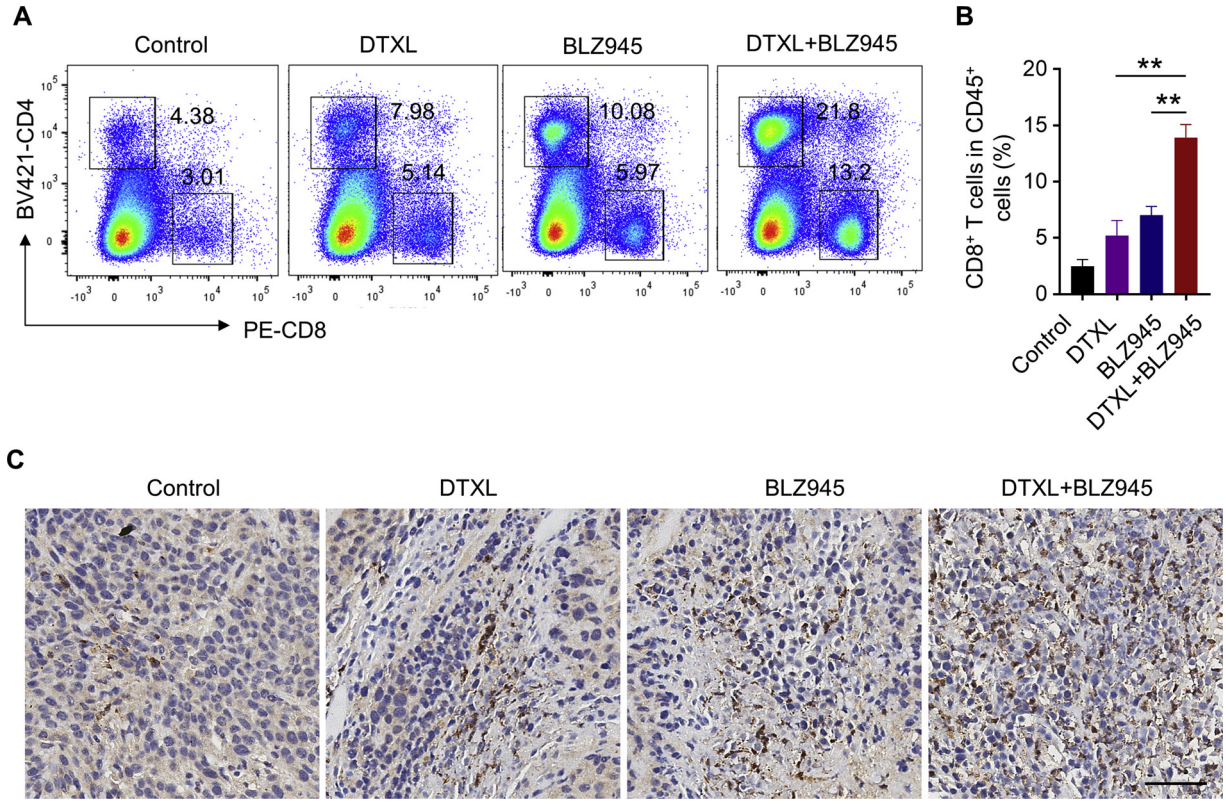

Fig. 4. Combination therapy enhances the infiltration of CD8 + T cells. (A) Relative abundance of CD8 + T cells in ID8 tumor tissues at the end of treatment examined by flow cytometry. (B) Bar graph shows the percentage of CD8 + T cells in tumor-infiltrating immune cells. Data are shown as means ± SD (n = 8). **p < 0.005. (C) The abundance of CD8 + T cells in tumor tissues examined by immunohistochemistry, the brown dots indicated CD8 + T cells. Scale bar, 50 μm.

treatment significantly decreased mRNA levels of TAM-associated genes Arg1, Mrc1 and IL-10 (Fig. 3E) compared to DTXL or BLZ945 single treatment, indicating DTXL and BLZ945 combination treatment reduced TAMs abundance. Taken together, our data demonstrated that DTXL and BLZ945 combination therapy significantly inhibited tumor growth and reduced the abundance of TAMs.

3.4. DTXL and BLZ945 combination therapy enhanced the infiltration of CD8$^+$ T cells

CD8$^+$ T cells are the key effector cell population mediating effective anti-tumor immunity to cancer (Huang et al., 2015). It has been described that TAMs impeded CD8$^+$ T cells infiltration and suppressed their activities (Cassetta and Kitamura, 2018; Peranzoni et al., 2018). We continued to evaluate the effect of DTXL/BLZ945 treatment on CD8$^+$ T cells infiltration by flow cytometry. DTXL/ BLZ945 combination treatment significantly increased the ratio of CD8$^+$ T in tumor tissues when compared to DTXL or BLZ945 single treatment (Fig. 4A and B). Similarly, by using immunohistochemistry staining, we also detected more CD8$^+$ T cells in tumor tissues from DTXL/BLZ945 combination-treated mice than that from DTXL or BLZ945 single-treated mice (Fig. 4C). Collectively, our data demonstrated that DTXL and BLZ945 combination treatment enhanced CD8$^+$ T cells infiltration.

3.5. DTXL and BLZ945 combination therapy significantly inhibited lung metastasis

TAMs have been implicated in cancer metastasis (Nielsen and Schmid, 2017; Zarif et al., 2014; Riabov et al., 2014). As DTXL/BLZ945 combination treatment inhibited TAMs infiltration, we continued to evaluate the effect on metastasis. Expression of vascular endothelial growth factor (VEGF) and matrix metalloproteinase (MMP) contribute to angiogenesis and metastasis (Mahecha and Wang, 2017; Zheng et al., 2006). First we examined the expression of VEGF and MMP9 in tumor tissues after treatment. DTXL single treatment did not obviously affect expression of VEGF. In contrast, BLZ945 treatment decreased VEGF expression level (Fig. 5A). Interestingly, DTXL/BLZ945 combination treatment had significantly decreased the VEGF level when compared to DTXL or BLZ945 single treatment. We got the similar result on MMP9 expression level (Fig. 5B). These results suggested that DTXL and BLZ945 combination treatment could inhibit metastasis. We next examined the lung metastasis. As shown in Fig. 5C, we detected obvious less metastatic tumor (dotted circle) in lung tissues from DTXL/BLZ945 combination-treated mice when compared to DTXL or BLZ945 single-treated mice. In addition, the area of metastatic tumor in DTXL/BLZ945 combination-treated mice was significantly smaller than that in DTXL or BLZ945 single-treated mice (Fig. 5D). Taken together, our data demonstrated that DTXL and BLZ945 combination treatment significantly inhibited lung metastasis.

4. Discussion

TAMs are the main population of inflammatory cells in solid tumors which possess diversified significance in tumor development. TAMs are derived from circulating monocytes and differentiate within the tumor microenvironment. TAMs generally display M2-like phenotype, fail to express pro-inflammatory cytokines while are excellent producers of immunosuppressive cytokines. Therefore, unlike M1 macrophages which have strong microbicidal and tumoricidal activities, M2-like TAMs are immunosuppressive and facilitate tumor progression (Allavena et al., 2008).

The chemo-resistance and radio-protective effects of TAMs have also been described. Increased density of TAMs is associated with poor efficacy in chemotherapy. DTXL is widely used to treat multiple cancers

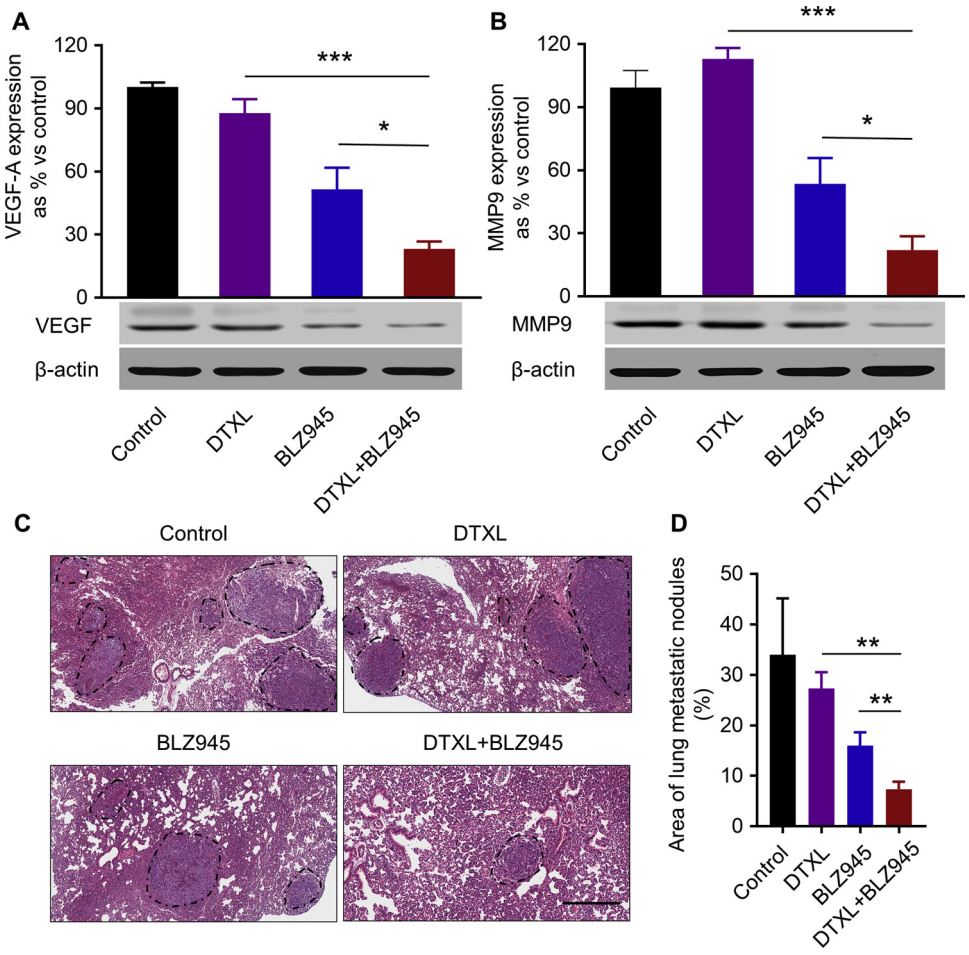

Fig. 5. Combination therapy significantly inhibits lung metastasis of ID8 ovarian tumor. (A–B) Relative mRNA and protein expressions of VEGF-A and MMP9. β-actin was used as the loading control. Data are shown as means ± SD (n = 8). *p < 0.05, ***p < 0.001. (C) Representative images of haematoxylin and eosin (H&E) staining of lung metastases from mice treated with different formulations. The dotted circle indicates a metastatic tumor. Scale bar, 50 μm. (D) Lung metastases were quantified as percentage of metastatic area per lung area. Data are shown as means ± SD (n = 8). **p < 0.005.

including ovarian cancer while the development of DTXL resistance has emerged (Hwang, 2012). Interestingly, in present study, we found that DTXL treatment increased the TAMs infiltration in ovarian tumor tissues, which could partially contribute to DTXL resistance.

CSF-1 and its receptor CSF-1R, regulated the migration, differentiation and survival of macrophages and their precursors (Hume and MacDonald, 2012). Inhibition of CSF-1R was able to deplete TAMs and inhibit their tumor-promoting function. In present study, we investigated the effect of CSF-1R inhibiting by BLZ945 and found BLZ945 inhibited CSF-1R signaling pathway and induced apoptosis on macrophages. TAMs have been shown to blunt chemotherapy-induced antitumor responses by secreting chemoprotective factors such as MMP-9 (De Palma and Lewis, 2013). Our data demonstrated that inhibiting of CSF-1R by BLZ945 decreased the MMP-9 level, decreased the expression of M2-related factors including mannose receptor-1 (Mrc1), arginase-1 (Arg1) and interleukin 10 (IL10). Most importantly, BLZ945 promoted the anti-tumor activity of DTXL as BLZ945 together with DTXL displayed the most robust inhibitory effect on ovarian tumor. Therefore, our data also confirmed that targeting of TAMs could be promising therapeutic approach for cancer treatment. In addition, the combination of BLZ945 with DTXL could be utilized as a rationale therapeutic treatment for cancer.

$CD8^+$ T cells play the key role in fighting against cancer. To kill tumor cells, T cells need to accumulate in the tumor and migrate efficiently to contact with malignant cells, and respond adequately to tumor antigens. Accumulating evidence has suggested that the total number of T cells found within a tumor is the key factor to influence the outcome of tumor development (Peranzoni, et al., 2018). However, poor representation of $CD8^+$ T cells in tumors is a fundamental hurdle to successful cancer treatment. Peranzoni et al described that $CD8^+$ T cells migrated poorly and invade tumor nests due to long-lasting interactions with TAMs in the stroma. Depletion of TAMs restored $CD8^+$ T cells migration and infiltration into tumor islets. In present study, we also demonstrated that administration of BLZ945 together with DTXL significantly increased the infiltration of $CD8^+$ T cells in tumor tissues, indicating depletion of TAMs resulted in increased $CD8^+$ T cell in tumor tissues and contributed to better tumor inhibition. The increased $CD8^+$ T cell infiltrations to tumor by inhibiting CSF1R have also been described in multiple studies. For example, by using a CSF1R neutralization antibody, Ries and colleagues reported that targeting of CSF1R results in a higher CD8/CD4 T cell ratio in tumor lesions in cancer patients (Ries et al., 2014).

TAMs has been reported to promote cancer progress and metastasis through the release of a variety of chemokines, inflammatory factors and growth factors (Qian and Pollard, 2010). Fang et al described that TAMs promoted the metastatic potential of thyroid papillary cancer by releasing CXCL8. Targeting TAMs by inhibiting either the CSF1R or CCR2 decreased the number of tumor-initiating cells (TIC) and inhibited metastasis (Mitchem et al., 2013). In present study, depletion of TAMs by BLZ945 also inhibited of lung metastasis and the combination of BLZ945 and DTXL displayed the best inhibition, which suggested BLZ945 could be a great supplementary to DTXL to treat cancer.

Overall, the current study demonstrated that depletion of TAMs by BLZ945 enhanced the anti-tumor effects of DTXL in the mice with epithelial ovarian cancer. However, it is still far away to apply BLZ945 in real clinic therapeutic treatment. Although BLZ945 did not cause obviously toxicity and was effective in mice, the safety and efficacy in human need to be evaluated and the dosage, suitable administration route of BLZ945 in human should be determined. Now the Phase I/II Study of BLZ945 are ongoing. Based on results from current animal studies, it should be promising to utilize BLZ945 as an cancer treatment.

5. Conclusion

We demonstrated that DTXL treatment resulted in increased TAMs in tumor tissue. Depletion of TAMs by BLZ945 enhanced the anti-tumor effect of DTXL.

Disclosure of potential conflicts of interest

The authors declare that they have no conflict of interest.

Acknowledgement

None.

References

Allavena, P., Sica, A., Solinas, G., Porta, C., Mantovani, A., 2008. The inflammatory micro-environment in tumor progression: the role of tumor-associated macrophages. Crit. Rev. Oncol. Hematol. 66, 1.

Al-Wahab, Z., Tebbe, C., Chhina, J., Dar, S.A., Morris, R.T., Ali-Fehmi, R., Giri, S., Munkarah, A.R., Rattan, R., 2014. Dietary energy balance modulates ovarian cancer progression and metastasis. Oncotarget 5, 6063.

Bonapace, L., Coissieux, M.M., Wyckoff, J., Mertz, K.D., Varga, Z., Junt, T., Bentires-Alj, M., 2014. Cessation of CCL2 inhibition accelerates breast cancer metastasis by promoting angiogenesis. Nature 515, 130.

Cassetta, L., Kitamura, T., 2018. Targeting tumor-associated macrophages as a potential strategy to enhance the response to immune checkpoint inhibitors. Front Cell Dev. Biol. 6, 38.

Dammeijer, F., Lievense, L.A., Kaijen-Lambers, M.E., van Nimwegen, M., Bezemer, K., Hegmans, J.P., van Hall, T., Hendriks, R.W., Aerts, J.G., 2017. Depletion of tumor-associated macrophages with a CSF-1R kinase inhibitor enhances antitumor immunity and survival induced by DC immunotherapy. Cancer Immunol. Res. 5, 535.

De Palma, M., Lewis, C.E., 2013. Macrophage regulation of tumor responses to anticancer therapies. Cancer Cell 23, 277.

DeNardo, D.G., Barreto, J.B., Andreu, P., Vasquez, L., Tawfik, D., Kolhatkar, N., Coussens, L.M., 2009. CD4(+) T cells regulate pulmonary metastasis of mammary carcinomas by enhancing protumor properties of macrophages. Cancer Cell 16, 91.

DeNardo, D.G., Brennan, D.J., Rexhepaj, E., Ruffell, B., Shiao, S.L., Madden, S.F., Gallagher, W.M., Wadhwani, N., Keil, S.D., Junaid, S.A., Rugo, H.S., Hwang, E.S., Jirstrom, K., West, B.L., Coussens, L.M., 2011. Leukocyte complexity predicts breast cancer survival and functionally regulates response to chemotherapy. Cancer Discov. 1, 54.

Guo, C., Buranych, A., Sarkar, D., Fisher, P.B., Wang, X.Y., 2013. The role of tumor-associated macrophages in tumor vascularization. Vasc Cell 5, 20.

Guppy, A.E., Nathan, P.D., Rustin, G.J., 2005. Epithelial ovarian cancer: a review of current management. Clin. Oncol. (R. Coll. Radiol.) 17, 399.

Huang, Y., Ma, C., Zhang, Q., Ye, J., Wang, F., Zhang, Y., Hunborg, P., Varvares, M.A., Hoft, D.F., Hsueh, E.C., Peng, G., 2015. CD4+ and CD8+ T cells have opposing roles in breast cancer progression and outcome. Oncotarget 6, 17462.

Hume, D.A., MacDonald, K.P., 2012. Therapeutic applications of macrophage colony-stimulating factor-1 (CSF-1) and antagonists of CSF-1 receptor (CSF-1R) signaling. Blood 119, 1810.

Hwang, C., 2012. Overcoming docetaxel resistance in prostate cancer: a perspective review. Ther. Adv. Med. Oncol. 4, 329.

Katsumata, N., 2003. Docetaxel: an alternative taxane in ovarian cancer. Br. J. Cancer 89 (Suppl.3), S9.

Kim, A., Ueda, Y., Naka, T., Enomoto, T., 2012. Therapeutic strategies in epithelial ovarian cancer. J. Exp. Clin. Cancer Res. 31, 14.

Mahecha, A.M., Wang, H., 2017. The influence of vascular endothelial growth factor-A and matrix metalloproteinase-2 and -9 in angiogenesis, metastasis, and prognosis of endometrial cancer. OncoTargets Ther. 10, 4617.

Mantovani, A., Marchesi, F., Malesci, A., Laghi, L., Allavena, P., 2017. Tumour-associated macrophages as treatment targets in oncology. Nat. Rev. Clin. Oncol. 14, 399.

Mitchem, J.B., Brennan, D.J., Knolhoff, B.L., Belt, B.A., Zhu, Y., Sanford, D.E., Belaygorod, L., Carpenter, D., Collins, L., Piwnica-Worms, D., Hewitt, S., Udupi, G.M., Gallagher, W.M., Wegner, C., West, B.L., Wang-Gillam, A., Goedegebuure, P., Linehan, D.C., DeNardo, D.G., 2013. Targeting tumor-infiltrating macrophages decreases tumor-initiating cells, relieves immunosuppression, and improves chemotherapeutic responses. Cancer Res. 73, 1128.

Nielsen, S.R., Schmid, M.C., 2017. Macrophages as key drivers of Cancer progression and metastasis. Mediators Inflamm. 2017, 9624760.

Peranzoni, E., Lemoine, J., Vimeux, L., Feuillet, V., Barrin, S., Kantari-Mimoun, C., Bercovici, N., Guerin, M., Biton, J., Ouakrim, H., Regnier, F., Lupo, A., Alifano, M., Damotte, D., Donnadieu, E., 2018. Macrophages impede CD8 T cells from reaching tumor cells and limit the efficacy of anti-PD-1 treatment. Proc. Natl. Acad. Sci. U. S. A. 115, E4041.

Pyonteck, S.M., Akkari, L., Schuhmacher, A.J., Bowman, R.L., Sevenich, L., Quail, D.F., Olson, O.C., Quick, M.L., Huse, J.T., Teijeiro, V., Setty, M., Leslie, C.S., Oei, Y., Pedraza, A., Zhang, J., Brennan, C.W., Sutton, J.C., Holland, E.C., Daniel, D., Joyce, J.A., 2013. CSF-1R inhibition alters macrophage polarization and blocks glioma progression. Nat. Med. 19, 1264.

Qian, B.Z., Pollard, J.W., 2010. Macrophage diversity enhances tumor progression and metastasis. Cell 141, 39.

Reid, B.M., Permuth, J.B., Sellers, T.A., 2017. Epidemiology of ovarian cancer: a review. Cancer Biol. Med. 14, 9.

Riabov, V., Gudima, A., Wang, N., Mickley, A., Orekhov, A., Kzhyshkowska, J., 2014. Role of tumor associated macrophages in tumor angiogenesis and lymphangiogenesis. Front. Physiol. 5, 75.

Richardsen, E., Uglehus, R.D., Johnsen, S.H., Busund, L.T., 2015. Macrophage-colony stimulating factor (CSF1) predicts breast cancer progression and mortality. Anticancer Res. 35, 865.

Ries, C.H., Cannarile, M.A., Hoves, S., Benz, J., Wartha, K., Runza, V., Rey-Giraud, F., Pradel, L.P., Feuerhake, F., Klaman, I., Jones, T., Jucknischke, U., Scheiblich, S., Kaluza, K., Gorr, I.H., Walz, A., Abiraj, K., Cassier, P.A., Sica, A., Gomez-Roca, C., de Visser, K.E., Italiano, A., Le Tourneau, C., Delord, J.P., Levitsky, H., Blay, J.Y., Ruttinger, D., 2014. Targeting tumor-associated macrophages with anti-CSF-1R antibody reveals a strategy for cancer therapy. Cancer Cell 25, 846.

Shen, K.Y., Song, Y.C., Chen, I.H., Chong, P., Liu, S.J., 2014. Depletion of tumor-associated macrophages enhances the anti-tumor immunity induced by a toll-like receptor agonist-conjugated peptide. Hum. Vaccin. Immunother. 10, 3241.

Sica, A., Schioppa, T., Mantovani, A., Allavena, P., 2006. Tumour-associated macrophages are a distinct M2 polarised population promoting tumour progression: potential targets of anti-cancer therapy. Eur. J. Cancer 42, 717.

Stanley, E.R., Chitu, V., 2014. CSF-1 receptor signaling in myeloid cells. Cold Spring Harb. Perspect. Biol. 6.

Tang, X., Mo, C., Wang, Y., Wei, D., Xiao, H., 2013. Anti-tumour strategies aiming to target tumour-associated macrophages. Immunology 138, 93.

Wolf, A.J., Arruda, A., Reyes, C.N., Kaplan, A.T., Shimada, T., Shimada, K., Arditi, M., Liu, G., Underhill, D.M., 2011. Phagosomal degradation increases TLR access to bacterial ligands and enhances macrophage sensitivity to bacteria. J. Immunol. 187, 6002.

Zarif, J.C., Taichman, R.S., Pienta, K.J., 2014. TAM macrophages promote growth and metastasis within the cancer ecosystem. Oncoimmunology 3, e941734.

Zheng, H., Takahashi, H., Murai, Y., Cui, Z., Nomoto, K., Niwa, H., Tsuneyama, K., Takano, Y., 2006. Expressions of MMP-2, MMP-9 and VEGF are closely linked to growth, invasion, metastasis and angiogenesis of gastric carcinoma. Anticancer Res. 26, 3579.